Observation-based variability in the global ocean carbon sink from 1959-2020

Val Bennington[1], Lucas Gloege[2], and Galen A McKinley[3]

[1]Lamont Doherty Earth Institute of Columbia University
[2]Columbia University
[3]Lamont Doherty Earth Observatory of Columbia University

November 22, 2022

Abstract

The ocean plays a critical role in reducing the human impact on the climate by absorbing and sequestering CO2. To quantify the ocean carbon sink, surface ocean pCO2; must be estimated across space and time. Sparse in situ pCO2; observations began in the 1980s, thus only global ocean biogeochemical models (GOBMs) have been the basis for quantification of the ocean carbon sink prior to the 1980s. The LDEO-Hybrid Physics Data product (LDEO-HPD) incorporates the physical knowledge within the GOBMs and corrects these estimates to observations. Here, we extend the LDEO-HPD product back to 1959 using a climatology of model-observation misfits. LDEO-HPD is closer to independent observations than unadjusted GOBMs. Most of the improvement from the GOBM prior in LDEO-HPD is attributable to the climatological adjustment, which supports the use of a climatological adjustment prior to 1982. Air-sea CO2; fluxes for 1959-2020 demonstrate response to atmospheric pCO2 growth and volcanic eruptions.

Observation-based variability in the global ocean carbon sink from 1959-2020

Val Bennington[1,2], Lucas Gloege[3], Galen A. McKinley[1]

[1]Lamont-Doherty Earth Observatory at Columbia University
[2]Makai Ocean Engineering, Inc.
[3]NASA-GISS

Key Points:

- A temporal extension of an observation-based product for surface ocean pCO_2 (LDEO-HPD) is presented.
- An XGB algorithm adjusts ocean models toward in situ data for 1982-2020; a climatological adjustment is applied for 1959-1981.
- The ocean carbon sink from 1959-2020 has responded to atmospheric pCO_2 growth and volcanic eruptions.

Corresponding author: Val Bennington, Valerie.Bennington@makai.com

Abstract

The ocean plays a critical role in reducing the human impact on the climate by absorbing and sequestering CO_2. To quantify the ocean carbon sink, surface ocean pCO_2 must be estimated across space and time. Sparse in situ pCO_2 observations began in the 1980s, thus only global ocean biogeochemical models (GOBMs) have been the basis for quantification of the ocean carbon sink prior to the 1980s. The LDEO-Hybrid Physics Data product (LDEO-HPD) incorporates the physical knowledge within the GOBMs and corrects these estimates to observations. Here, we extend the LDEO-HPD product back to 1959 using a climatology of model-observation misfits. LDEO-HPD is closer to independent observations than unadjusted GOBMs. Most of the improvement from the GOBM prior in LDEO-HPD is attributable to the climatological adjustment, which supports the use of a climatological adjustment prior to 1982. Air-sea CO_2 fluxes for 1959-2020 demonstrate response to atmospheric pCO_2 growth and volcanic eruptions.

Plain Language Summary

The ocean removes carbon dioxide (CO_2) from the atmosphere and reduces climate change caused by humans. The magnitude of this removal can be estimated using computer models of ocean physics, chemistry, and biology, as well as statistical extrapolations of observations. The observational record is too sparse to directly reconstruct air-sea fluxes prior to 1982, but by combining models and a statistical approach, we make an estimate for 1959-present that is substantially informed by observations. The LDEO-HPD product for air-sea CO_2 exchange includes two periods, with the first previously published for 1982-2020 and the second being this extension back in time. For 1959 to 1981, LDEO-HPD corrects models using the average of data-based corrections derived from the observed period. The LDEO-HPD product agrees much better with independent observations than the models alone, and can be used to understand what controls year to year changes in the ocean carbon sink.

1 Introduction

By absorbing and sequestering carbon dioxide from the atmosphere, the global oceans play a critical role in modulating climate change. The ocean has absorbed 37% of fossil carbon emissions since the start of the industrial age (Friedlingstein et al., 2021). Quantifying the distribution of carbon emissions across the land biosphere, oceans, and atmosphere is an important support to climate policy (Peters et al., 2017). In order to estimate air-sea fluxes of carbon dioxide, the driver of these fluxes, the partial pressure of carbon dioxide in the surface waters (pCO_2), must be estimated.

Global ocean biogeochemical models (GOBMs) explicitly model the physics, biology and chemistry of the ocean carbonate system and resulting pCO_2. Observation-based products utilize sparse observations of the partial pressure of CO_2 (pCO_2) from the Surface Ocean CO_2 ATlas (SOCAT) (Bakker et al., 2016), and train a machine learning algorithm to relate these data to full-coverage observations of associate variables such that pCO_2 can be estimated at all points in space and time. Although the resulting statistical models often do not explicitly include the known physics of the ocean carbonate system, the results compare well to independent observations of pCO_2 (Gregor et al., 2019; Denvil-Sommer et al., 2019; Landschützer et al., 2014; Bennington et al., 2022). The mixed layer model of Rodenbeck et al. (2013, 2021) does incorporate some physical processes, differing from the other machine learning based products.

While both global ocean biogeochemical models (GOBMs) and observation-based products are used to estimate this air-sea gas exchange of CO_2 for the recent historical period, observation-based products have been limited to the period of in situ observations that began in the 1980s. Eight GOBMs were used to quantify the historical air-

Table 1. Global Ocean Biogeochemical Models (GOBMs) and their corresponding references.

Global ocean biogeochemical model	Reference
CESM-ETHZ	Doney et al. (2009)
FESCOM2-REcoM	Gurses et al. (2021)
MICOM-HAMOCC (NorESM1-OCv1.2)	Schwinger et al. (2016)
MOM6-COBALT (Princeton)	Adcroft et al. (2019)
MPIOM-HAMOCC6 (MPI)	Paulsen et al. (2017)
NEMO-PlankTOM5	Buitenhuis et al. (2013)
NEMO-PISCES (IPSL)	Aumont et al. (2015)
NEMO3.6-PISCESv2-gas (CNRM)	Berthet et al. (2019)

sea CO_2 flux prior to the 1980s in the Global Carbon Budget 2021 (Friedlingstein et al., 2021). To incorporate the physical knowledge contained within GOBMs, Gloege et al. (2022) utilized the machine-learning algorithm XGBoost (Chen & Guestrin, 2016) to learn model-observation misfits of simulated surface ocean pCO_2. The resulting data product (LDEO-HPD) showed an improved fit compared to the independent data over other data products. The resulting historical reconstruction of air-sea CO_2 fluxes from the extended LDEO-HPD is within the range of other data products, and in agreement with 2010-2020 mean flux estimates from the Global Carbon Budget 2021 (Friedlingstein et al., 2021).

LDEO-HPD estimated air-sea fluxes beginning in 1982. Here, we extend LDEO-HPD back in time by applying the climatology of 2000-2020 estimated GOBM-observation misfits to the GOBMs for 1959-1981. As discussed below, this approach is supported by the fact that much of the skill in LDEO-HPD against independent modern observations is due to the climatological correction.

This paper is organized as follows. We present the methods and resulting estimated air-sea CO_2 fluxes for 1959-2020. We then briefly examine the resulting estimated flux variability in four basins and globally.

2 Methods

The LDEO-HPD data product (Gloege et al., 2022) utilizes the nearly global coverage of satellite sea surface temperature (SST) (Reynolds et al., 2002), sea surface salinity (SSS) (Good et al., 2013), chlorophyll-a (Maritorena et al., 2010), geographic location, time of year, the climatology of mixed layer depth (de Boyer Montégut et al., 2004), and the machine learning algorithm XGBoost (Chen & Guestrin, 2016) to create a non-linear function between observations and the model-data misfit of surface ocean pCO_2. For the LDEO-HPD global reconstruction (1982-2020), misfits are calculated for each of eight (8) GOBMs to observed ocean surface pCO_2 (Bakker et al., 2016). Then, each of the GOBMs are independently adjusted with these corrections, which is unique to each GOBM. Finally, the average of the eight adjusted GOBMs is the final pCO_2 estimate. The GOBMs used here are the same as used in the Global Carbon Budget 2021 (Friedlingstein et al., 2021) (Table 1). The resulting model-data misfits are resolved at 1^o latitude by 1^o longitude for each month. The complete description of the LDEO-HPD method and the resulting data product are detailed in Gloege et al. (2022).

2.1 Climatology of Model-Data Misfit

Given the lack of surface ocean pCO_2 observations prior to the 1980s, we must determine what corrections (model-data misfits) to apply to the models prior to 1982. Ex-

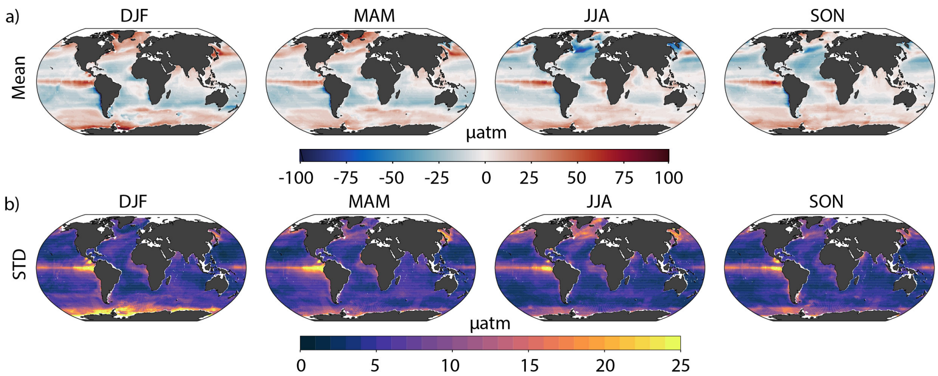

Figure 1. (a) Seasonal climatology (2000-2020) of model-data misfit in the Princeton model according to HPD. (b) Standard deviation of model-data misfit over 2000-2020 in the Princeton model, by season.

tending the analysis of climatological misfits by Gloege et al. (2022), we examine the interannual variability of the misfits for 2000-2020. We choose this period to best capture interannual variability (Bennington et al., 2022) since chlorophyll-a observations do not start until 1998 and a climatology of chlorophyll-a must be used prior (Landschützer et al., 2014).

The seasonal climatology and standard deviation of the model-data misfit for the Princeton GOBM is a representative example of the climatological misfit (Figure 1). Mean misfits are large in all seasons in the subpolar, equatorial, and Southern Ocean regions (Figure 1a). Interannual variability in the model-data misfit is quantified as the misfit standard deviation (Figure 1b). Year-to-year changes in misfits are significantly smaller in magnitude than the mean, typically less than 5 μatm. Larger standard deviations can occur during the biologically productive seasons in the subpolar regions and Southern Ocean. The equatorial Pacific exhibits moderate interannual variability in all seasons. These patterns of misfit and variability are similar across most of the ocean models (Supplementary), excepting MPIOM-HAMOCC (Gloege et al., 2022).

Since interannual variability in the reconstructed model-data misfit is generally small compared to the misfit mean, our approach to extending LDEO-HPD to the beginning of the model simulations is to use the monthly climatology of the 2000-2020 model-data misfit as the 1959-1981 correction for the GOBMs. This correction is separately calculated for, and applied to, each of eight GOBMs. The final pCO_2 reconstruction is the ensemble mean of the eight corrected GOBM pCO_2 estimates (modeled pCO_2 + reconstructed correction).

Table 2. Observation-based products (Fay et al., 2021) and their corresponding references.

Data Product	Reference
LDEO-HPD	Gloege et al. (2022), this paper
JENA MLS	Rödenbeck et al. (2021)
CSIR ML6	Gregor et al. (2019)
MPI SOMFFN	Landschützer et al. (2014)
CMEMS FFNN	Denvil-Sommer et al. (2019)
pCO_2 Residual	Bennington et al. (2022)

To assess how interannual variability is impacted by the climatological correction, comparison to independent data is required. These data do not exist in sufficient number for the 1959-1981 period, but do exist after 1990. Thus, we create an alternative reconstruction, $HPD_{ClimatologyTest}$, that applies the climatology of the model-data misfit for 2000-2020 to the entire reconstruction period (1959-2020). With $HPD_{ClimatologyTest}$, we can assess the impact of a climatological correction on the interannual variability of the reconstruction.

Figure 2 compares the original uncorrected GOBMs (squares), and five observation-based products (crosses) to GLODAP and LDEO observations for 1990-2020. The observation-based products all have substantially greater skill than the uncorrected GOBMs. $HPD_{ClimatologyTest}$ (solid blue diamond) has similar skill as the suite of observation-based products (Figure 2). This leads to an important finding, which is that most of LDEO-HPD's skill is due to the correction of the GOBM's climatological mean state and seasonality (Fay & McKinley, 2021) rather than their interannual variability. The additional skill achieved by adding interannual variability to the corrections (1) is shown by the difference between $HPD_{ClimatologyTest}$ and LDEO-HPD, which is modest for GLODAP (Figure 2a) and slightly larger for LDEO (Figure 2b). This additional increment of skill brings LDEO-HPD closest to the independent observations of these currently-available observation-based products (Gloege et al., 2022).

2.2 CO_2 Flux Calculations

In the previous comparisons, we consider pCO_2. To assess the global ocean carbon sink associated with these pCO_2 estimates, air-sea CO_2 exchange must be calculated. We use the same gas transfer velocity, solubility, winds, and ice for LDEO-HPD, other observation-based products, and the GOBMs so that differences in these calculations do not factor into the resulting comparison (Fay et al., 2021). EN4.2.2 salinity (Good et al., 2013); ERA5 winds, sea level pressure, and sea surface temperature; (Bell et al., 2020, 2019); the wind scaling factor for ERA5 (Gregor & Fay, 2021); and Hadley sea ice fractional coverage (Rayner et al., 2003) are used. Unreconstructed coastal areas in data products are filled with the scaled coastal pCO_2 climatology (Landschützer et al., 2020), also following Fay et al. (2021).

Air-sea CO_2 flux (FCO_2) is estimated using a bulk parameterization (Equation 1),

$$FCO_2 = K_w \cdot K0 \cdot (1 - ice_{fraction}) \cdot (pCO_2^{sea} - pCO_2^{atm}) \tag{1}$$

where K_w is the gas-transfer velocity calculated from wind speeds, scaled to the 16.5 cm/hr 14C bomb flux estimate according to Wanninkhof (1992) and Sweeney et al. (2007) as in Gregor and Fay (2021); K0 is the solubility calculated using salinity and SST; pCO_2^{atm} is the water vapor corrected atmospheric partial pressure of CO_2 from CarboScope (Rödenbeck, 2005); and pCO_2^{sea} is the surface ocean pCO_2.

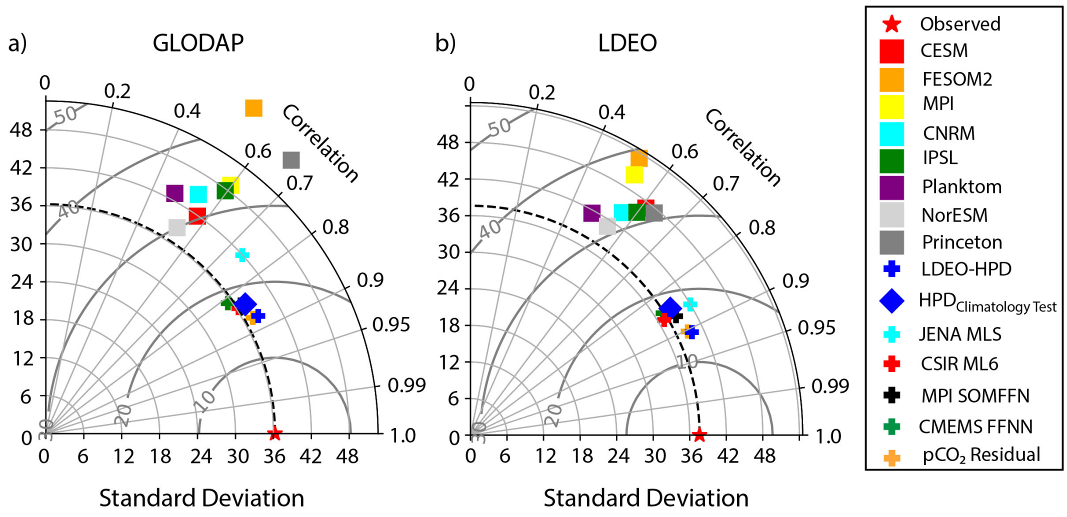

Figure 2. Taylor diagrams (Taylor, 2001) depict the skill of each ocean model (squares), previous data products (crosses), LDEO-HPD (blue cross), and $\mathrm{HPD}_{ClimatologyTest}$. The ability to capture observed pCO_2 variability for 1990-2020 is evaluated against two global datasets (a) GLODAP and (b) LDEO. The red star indicates the standard deviation of each dataset. Distance along the radius represents the ability to capture observed variability (standard deviation). The distance along the circumference depicts correlation with the observations, and grey inlaid circles show unbiased RMSE compared to the observations.

Data products which incorporate observations of surface ocean pCO_2 include both natural and anthropogenic carbon in the resulting pCO_2 and CO_2 flux product. This is the net CO_2 flux ($F_{net} = F_{natural} + F_{ant}$). Global ocean biogeochemical models exclude the natural outgassing of riverine carbon ($F_{natural}$), which caused net CO_2 efflux from the preindustrial ocean (Aumont et al., 2001). To quantify the anthropogenic air-sea CO_2 flux, this $F_{natural}$ must be subtracted from our net flux, given that the models have been corrected toward pCO_2 observations consistent with F_{net}. Quantifying the global air-sea CO_2 flux due to decomposition and outgassing of riverine carbon remains uncertain and is the topic of current research. Here, as in Gloege et al. (2022) and Bennington et al. (2022), we use an average of three estimates: Jacobson et al. (2007): (0.45 +/- 0.18 PgC/yr), Resplandy et al. (2018): (0.78 +/- 0.41 PgC/yr), and Lacroix et al. (2020): (0.23 Pg C / yr). The combined estimated efflux due to riverine carbon is 0.49 +/- 0.26 Pg C/yr, and we remove the efflux of 0.49 PgC/yr from the estimated annual air-sea CO_2 fluxes calculated using the LDEO-HPD and other data products' pCO_2.

2.3 Box model

The box model of McKinley et al. (2020) estimates the global-mean air-sea CO_2 flux that occurs in response to the observed growth of atmospheric pCO_2. It also has the option to include upper ocean heat content anomalies driven by the 3 most climatically impactful volcanic eruptions of the last 60 years: Agung in 1963, El Chichon in 1982, and Mt Pinatubo in 1991 (Crisp et al., 2021). Comparing air-sea CO_2 fluxes estimated by the box model for 1960-2019 allows consideration of flux variability with and without large volcanic influences and puts LDEO-HPD into context with previous comparisons of the box model to observation-based products (McKinley et al., 2020).

3 Results

3.1 CO_2 Fluxes

Air-sea CO_2 fluxes for 1959-2020 from LDEO-HPD, the eight GOBMs, previously published observation-based products, and $HPD_{ClimatologyTest}$ demonstrate a long-term increasing trend punctuated by interannual variability (Figure 3a). There most significant feature of this variability is the slowed growth in uptake during the 1990s (Le Quéré et al., 2007; Lovenduski et al., 2007, 2008; Fay & McKinley, 2013; Landschützer et al., 2015).

In LDEO-HPD, interannual variability prior to 1982 is driven by only the GOBMs; only the mean flux and seasonality have been adjusted with climatological model-data misfits. The adjustment leads to a larger mean flux than most of the GOBMs (Figure 3a). From 1982 onward, the flux in LDEO-HPD is very similar to $HPD_{ClimatologyTest}$, but has larger extremes. These differences are due to the interannually varying adjustments that are possible only during the observed period. This comparison indicates that LDEO-HPD likely underestimates the amplitude of interannual anomalies prior to 1982, which is to be expected when there are no data to directly drive the reconstruction toward extremes (Rödenbeck et al., 2021).

Examining the spatial patterns of the mean air-sea carbon dioxide fluxes for each 20 year period in Figure 3b, we see a reduced Pacific equatorial efflux during 1980-1999 compared to the other periods, consistent with the occurrence of multiple strong El Niño events in this period (e.g. 1982-83, 1997-98). In the Northern extratropics, the sink strengthens over time.

Integrated flux anomalies at each latitude reveal the spatial distribution of interannual anomalies (Figure 4). Consistent with the global timeseries (Figure 3a), the dominant feature is the long-term growth (red to blue) of the ocean carbon sink at all latitudes.

The Pacific Ocean has large integrated flux variability, with significant anomalies occurring on interannual timescales within the equatorial region as a result of ENSO (McKinley et al., 2004, 2017; Rödenbeck et al., 2021). The Southern Ocean experiences significant carbon sink decadal variations (Le Quéré et al., 2007; Lovenduski et al., 2007, 2008; Landschützer et al., 2015, 2016; Ritter et al., 2017; McKinley et al., 2017; Gruber et al., 2019). Significant negative anomalies (greater uptake) occur in the 1980s to early 1990s, with anomalies of greatest intensity in 1992-93. After 1997, a strong positive anomaly (reduced uptake) emerges and extends for about a decade. From 2009 on, the anomaly is again negative in the Southern Ocean. These decadal variations remain after detrending the air-sea fluxes (Figure S2). In the Atlantic, latitudes north of 40^oN have the most intense fluxes. This basin is narrower than the others, and thus has a lower integrated flux and lower amplitude interannual variability. The Indian Ocean exhibits significant variability south of 10^oS according to the reconstruction; however the region is particularly sparse in observations to guide the reconstruction, which should increase its uncertainty (Gloege et al., 2021).

Increased uptake occurs in the Pacific and Southern Oceans immediately following the eruptions of Agung (March 1963), El Chichon (March 1982) and Mt. Pinatubo (June 1991). These can also be seen in the detrended flux anomalies (Figure S2). In the equatorial Pacific, the El Niño events that tend to follow these eruptions drive significant flux anomalies (Eddebbar et al., 2019). After El Chichon and Pinatubo, slight negative anomalies also occur in the Southern Hemisphere Atlantic. The globally-averaged box model of McKinley et al. (2020) parameterizes these eruptions as upper ocean heat content anomalies; the estimated fluxes correlate highly with LDEO-HPD (Figure S1d, r=0.82). If the eruptions are neglected, the correlation decreases (r=0.64). When both timeseries are detrended, the correlations remain significant only when the eruptions are

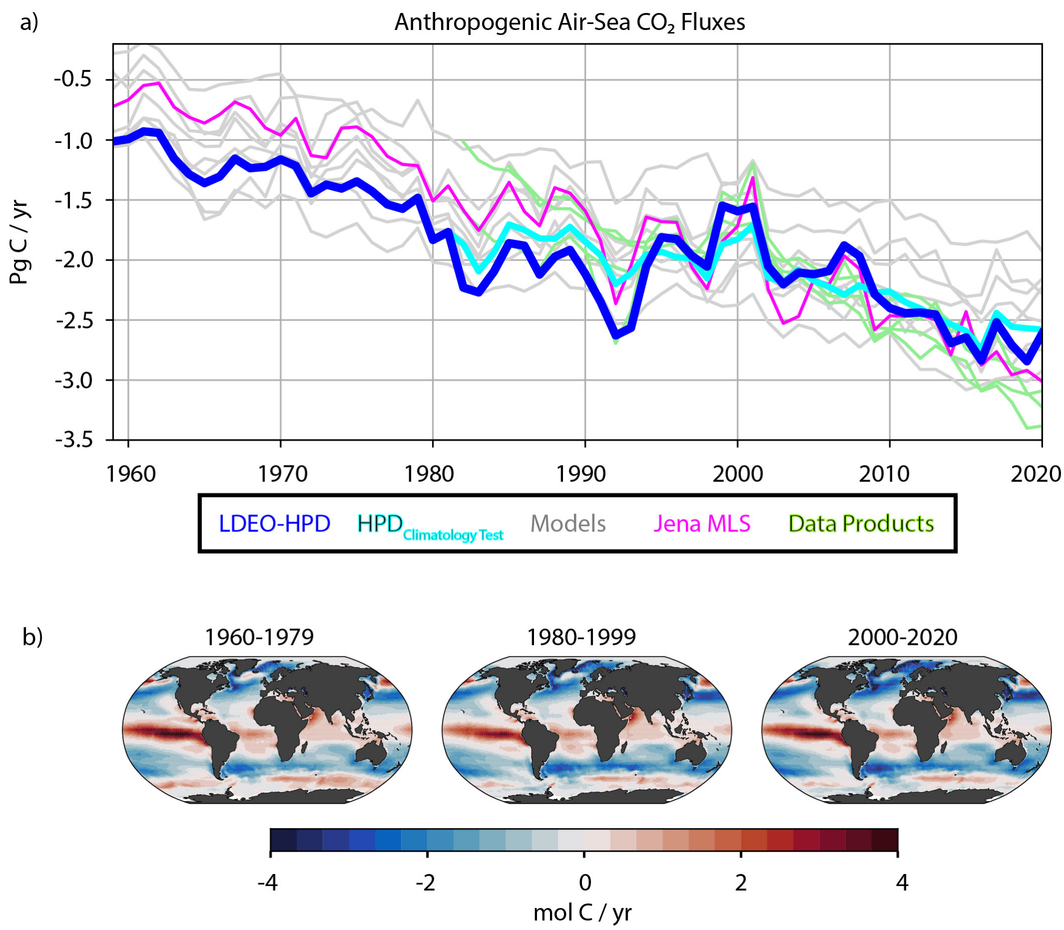

Figure 3. (a) Estimated air-sea CO_2 fluxes for 1959-2020 (Pg C/yr): LDEO-HPD (blue), $HPD_{ClimatologyTest}$ (cyan), unadjusted GOBMs (grey), Jena MLS (magenta), other observation-based products (green); comparisons shown in separate panels in Figure S1. $HPD_{ClimatologyTest}$ is identical to LDEO-HPD prior to 1982. (b) Map of mean air-sea CO_2 fluxes for 1960-1979, 1980-1999, and 2000-2020 according to LDEO-HPD (mol C / yr).

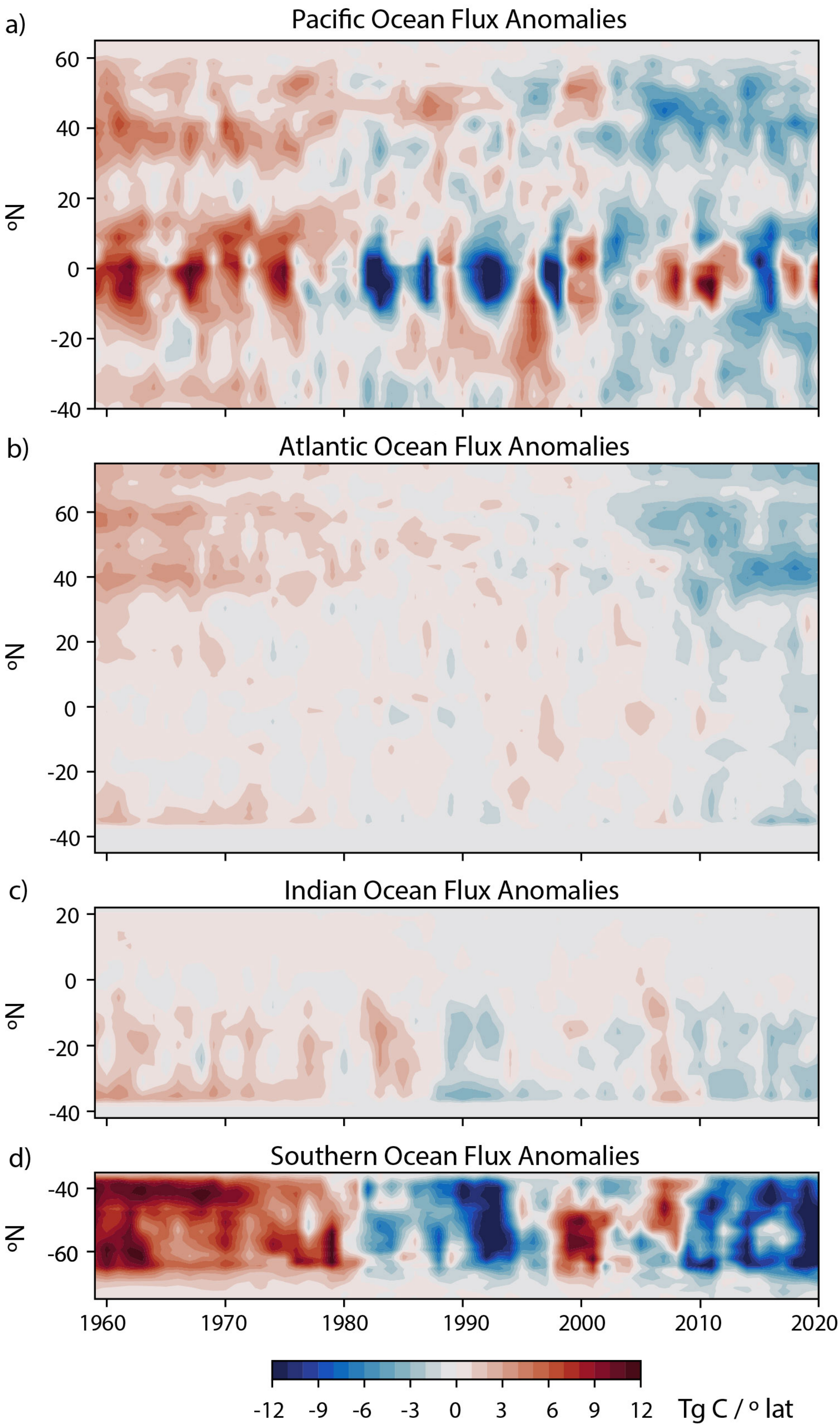

Figure 4. Air-sea CO_2 flux anomalies in four ocean basins (TgC/yr/^{o}lat).

included in the box model (with eruptions, $r=0.51$, $p<0.05$; without, $r=-0.23$, $p=0.13$). Thus, both the box model and the spatial patterns of flux anomalies (Figure 4) indicates the potential for large volcanoes to impact interannual variability of the global ocean carbon sink since 1959. A more detailed study of this issue in the LDEO-HPD product will be presented elsewhere.

4 Discussion and Conclusions

This work temporally extends the LDEO-HPD data product back in time to begin in 1959. For 1982-2020, model-data misfits are calculated for each model and each month as in Gloege et al. (2022). For 1959-1981, the monthly climatology of this correction for 2000-2020 is applied independently to each of eight GOBMs. Across all years, the final LDEO-HPD pCO_2 estimate is the average across the eight corrected models.

In comparison to independent data in the modern era, we find that the substantial improvement over uncorrected GOBMs is due primarily to the correction of the model mean and seasonality; i.e. the climatological correction. There are significant regional biases in the mean and seasonality of many GOBMs (Fay & McKinley, 2021; Hauck et al., 2020), and this observation-based approach can substantially improve these biases to bring the resulting estimates closer to observations (Figure 2). At the same time, this approach can preserve the GOBMs capability to represent interannual variability (Figure 3) that occurs in response to external forcing and internal ocean processes. By combining the strengths of models and observations with the LDEO-HPD approach, we have developed a robust approach to temporally extend this observation-based product back to 1959.

Compared to another recently developed extension, Jena MLS (Rödenbeck et al., 2021), the two sink estimates are significantly correlated ($r=0.93$, $p=0$ and $r=0.66$, $p=0$ when series are detrended). The two reconstructions span the range of model flux estimates prior to 1990s (Figure 3b), after which observations better constrain the products. Jena-MLS has a significantly larger estimated trend in the ocean carbon sink over the reconstructed period. However, as discussed by Rödenbeck et al. (2021) (their section A2), Jena-MLS in its current version overestimates the flux trend; thus, it likely underestimates the sink for the pre-observation decades.

LDEO-HPD indicates that the ocean carbon sink increased over the last 60 years, due to the long-term growth of atmospheric pCO_2 (Raupach et al., 2014; McKinley et al., 2020; Ridge & McKinley, 2021). Long-term growth is punctuated by year-to-year variability. Consistent with many earlier studies, the equatorial Pacific and Southern Ocean have the largest integrated impact on variations of the sink (Le Quéré et al., 2003; McKinley et al., 2004; Resplandy et al., 2015; McKinley et al., 2017; Landschützer et al., 2016; Hauck et al., 2020). The timing of these changes is consistent with ENSO variability in the equatorial Pacific. The Southern Ocean exhibits strong decadal timescale variations for which both internal and externally-forced mechanisms have been proposed. Better understanding the variability of ocean carbon uptake in the Southern Ocean and across the globe is an important task that can be facilitated by observation-based products such as LDEO-HPD.

Acknowledgments

The authors acknowledge support from NOAA (NA20OAR4310340) and the Data Science Institute of Columbia University. L.G was sponsored by the National Aeronautics and Space Administration (NASA) through a contract with ORAU. The views and conclusions contained in this document are those of the authors and should not be interpreted as representing the official policies, either expressed or implied, of the National Aeronautics and Space Administration (NASA) or the U.S. Government. The U.S.Government is authorized to reproduce and distribute reprints for Government purposes notwithstanding any copyright notation herein. We acknowledge that all data providers and quality controllers who work tirelessly to maintain the SOCAT database. We also acknowledge the ocean biogeochemical modelers who contribute to the Global Carbon Budget for sharing their output with us; and we thank J. Hauck specifically for her leadership on this effort. EN.4.2.2 data were obtained from https://www.metoffice.gov.uk/hadobs/en4/ and are © British Crown Copyright, Met Office, [2022], provided under a Non-Commercial Government Licence:

`http://www.nationalarchives.gov.uk/doc/non-commercial-government-licence/version/2/`.

Project code available at: `https://github.com/valbennington/LDEO_HPD_extension`.

References

Adcroft, A., Anderson, W., Balaji, V., Blanton, C., Bushuk, M., Dufour, C. O., ... Zhang, R. (2019). The GFDL Global Ocean and Sea Ice Model OM4.0: Model description and simulation features. *Journal of Advances in Modeling Earth Systems*, *11*(10), 3167-3211. doi: https://doi.org/10.1029/2019MS001726

Aumont, O., Ethé, C., Tagliabue, A., Bopp, L., & Gehlen, M. (2015). PISCES-v2: An ocean biogeochemical model for carbon and ecosystem studies. *Geoscientific Model Development*, *8*, 2465–2513. doi: 10.5194/gmd-8-2465-2015

Aumont, O., Orr, J. C., Monfray, P., Ludwig, W., Amiotte-Suchet, P., & Probst, J.-L. (2001). Riverine-driven interhemispheric transport of carbon. *Global Biogeochemical Cycles*, *15*(2), 393-405. doi: https://doi.org/10.1029/1999GB001238

Bakker, D. C. E., Pfeil, B., Landa, C. S., Metzl, N., O'Brien, K. M., Olsen, A., ... Xu, S. (2016). A multi-decade record of high-quality fCO_2 data in version 3 of the Surface Ocean CO_2 Atlas (SOCAT). *Earth System Science Data*, *8*(2), 383–413. doi: 10.5194/essd-8-383-2016

Bell, B., Hersbach, H., Berrisford, P., Dahlgren, P., Horányi, A., Muñoz Sabater, J., ... Thépaut, J.-N. (2019). *ERA5 monthly averaged data on single levels from 1979 to present.* Copernicus Climate Change Service (C3S) Climate Data Store (CDS). doi: 10.24381/cds.f17050d7

Bell, B., Hersbach, H., Berrisford, P., Dahlgren, P., Horányi, A., Muñoz Sabater, J., ... Thépaut, J.-N. (2020). *ERA5 monthly averaged data on single levels from 1950 to 1978 (preliminary version).* Copernicus Climate Change Service (C3S) Climate Data Store (CDS).

Bennington, V., Galjanic, T., & McKinley, G. A. (2022). Estimating historical air-sea CO_2 fluxes: Incorporating physical knowledge within a data-only approach. *Journal of Advances in Modeling Earth Systems*, *In Review.* Retrieved from `https://doi.org/10.1002/essoar.10510196.1`

Berthet, S., Séférian, R., Bricaud, C., Chevallier, M., Voldoire, A., & Ethé, C. (2019). Evaluation of an online grid-coarsening algorithm in a global eddy-admitting ocean biogeochemical model. *Journal of Advances in Modeling Earth Systems*, *11*(6), 1759-1783. doi: https://doi.org/10.1029/2019MS001644

Buitenhuis, E. T., Hashioka, T., & Quéré, C. L. (2013). Combined constraints on global ocean primary production using observations and models. *Global Biogeochemical Cycles*, *27*(3), 847-858. doi: https://doi.org/10.1002/gbc.20074

Chen, T., & Guestrin, C. (2016). Xgboost: A scalable tree boosting system. *CoRR*, *abs/1603.02754*.

Crisp, D., Dolman, H., Tanhua, T., McKinley, G. A., Hauck, J., Eggleston, S., & Aich, V. (2021). How well do we understand the land-ocean-atmosphere carbon cycle? *Reviews in Geophysics*, *in review*. doi: 10.1002/essoar.10506293.2

de Boyer Montégut, C., Madec, G., Fischer, A. S., Lazar, A., & Iudicone, D. (2004). Mixed layer depth over the global ocean: An examination of profile data and a profile-based climatology. *Journal of Geophysical Research: Oceans*, *109*(C12). doi: https://doi.org/10.1029/2004JC002378

Denvil-Sommer, A., Gehlen, M., Vrac, M., & Mejia, C. (2019). LSCE-FFNN-v1: a two-step neural network model for the reconstruction of surface ocean pCO2 over the global ocean. *Geoscientific Model Development*, *12*, 2091–2105. doi: https://doi.org/10.5194/gmd-12-2091-2019

Doney, S. C., Lima, I., Feely, R. A., Glover, D. M., Lindsay, K., Mahowald, N., ... Wanninkhof, R. (2009). Mechanisms governing interannual variability in upper-ocean inorganic carbon system and air–sea CO_2 fluxes: Physical climate and atmospheric dust. *Deep Sea Research Part II: Topical Studies in Oceanography*, *56*(8), 640-655. doi: https://doi.org/10.1016/j.dsr2.2008.12.006

Eddebbar, Y. A., Rodgers, K. B., Long, M. C., Subramanian, A. C., Xie, S.-P., & Keeling, R. F. (2019). El niño–like physical and biogeochemical ocean response to tropical eruptions. *Journal of Climate*, *32*(9), 2627 - 2649. doi: 10.1175/JCLI-D-18-0458.1

Fay, A. R., Gregor, L., Landschützer, P., McKinley, G. A., Gruber, N., Gehlen, M., ... Zeng, J. (2021). SeaFlux: harmonization of air–sea CO_2 fluxes from surface $p\mathrm{CO_2}$ data products using a standardized approach. *Earth System Science Data*, *13*(10), 4693–4710. doi: 10.5194/essd-13-4693-2021

Fay, A. R., & McKinley, G. A. (2013). Global trends in surface ocean pCO2 from in situ data. *Global Biogeochemical Cycles*, *27*(2), 541–557.

Fay, A. R., & McKinley, G. A. (2021). Observed regional fluxes to constrain modeled estimates of the ocean carbon sink. *Geophysical Research Letters*, *48*(20), e2021GL095325.

Friedlingstein, P., Jones, M. W., O'Sullivan, M., Andrew, R. M., Bakker, D. C., Hauck, J., ... others (2021). Global carbon budget 2021. *Earth System Science Data Discussions*, 1–191.

Gloege, L., McKinley, G. A., Landschützer, P., Fay, A. R., Frölicher, T. L., Fyfe, J. C., ... Takano, Y. (2021). Quantifying errors in observationally based estimates of ocean carbon sink variability. *Global Biogeochemical Cycles*, *35*(4), e2020GB006788. doi: https://doi.org/10.1029/2020GB006788

Gloege, L., Yan, M., Zheng, T., & McKinley, G. A. (2022). Improved quantification of ocean carbon uptake by using machine learning to merge global models and $p\mathrm{CO_2}$ data. *Journal of Advances in Modeling Earth Systems*, *14*. doi: 10.1029/2021ms002620

Good, S. A., Martin, M. J., & Rayner, N. A. (2013). EN4: Quality controlled ocean temperature and salinity profiles and monthly objective analyses with uncertainty estimates. *Journal of Geophysical Research: Oceans*, *118*(12), 6704-6716. doi: https://doi.org/10.1002/2013JC009067

Gregor, L., & Fay, A. (2021). *SeaFlux: harmonised sea-air CO2 fluxes from surface pCO2 data products using a standardised approach.* Zenodo. doi: 10.5281/zenodo.5482547

Gregor, L., Lebehot, A. D., Kok, S., & Monteiro, P. M. S. (2019). A comparative assessment of the uncertainties of global surface ocean CO_2 estimates using a machine-learning ensemble (CSIR-ML6 version 2019a) – have we hit the wall? *Geoscientific Model Development*, *12*, 5113–5136. doi: https://doi.org/10.5194/gmd-12-5113-2019

Gruber, N., Landschützer, P., & Lovenduski, N. S. (2019). The variable southern ocean carbon sink. *Annual Review of Marine Science*, *11*(1), 159-186. doi: 10

.1146/annurev-marine-121916-063407

Gurses, O., Hauck, J., Zeising, M., & Oziel, L. (2021). Global ocean biogeochemical modelling with FESOM2-REcoM. In *EGU General Assembly Conference Abstracts* (pp. EGU21–14980).

Hauck, J., Zeising, M., Le Quéré, C., Gruber, N., Bakker, D. C. E., Bopp, L., ... Séférian, R. (2020). Consistency and challenges in the ocean carbon sink estimate for the global carbon budget. *Frontiers in Marine Science*(7). doi: 10.3389/fmars.2020.571720

Jacobson, A. R., Mikaloff Fletcher, S. E., Gruber, N., Sarmiento, J. L., & Gloor, M. (2007). A joint atmosphere-ocean inversion for surface fluxes of carbon dioxide: 1. methods and global-scale fluxes. *Global Biogeochemical Cycles*, *21*(1). doi: https://doi.org/10.1029/2005GB002556

Lacroix, F., Ilyina, T., & Hartmann, J. (2020). Oceanic CO_2 outgassing and biological production hotspots induced by pre-industrial river loads of nutrients and carbon in a global modeling approach. *Biogeosciences*, *17*(1), 55-88.

Landschützer, P., Gruber, N., & Bakker, D. C. E. (2016). Decadal variations and trends of the global ocean carbon sink. *Global Biogeochemical Cycles*, *30*(10), 1396-1417. doi: https://doi.org/10.1002/2015GB005359

Landschützer, P., Gruber, N., Bakker, D. C. E., & Schuster, U. (2014). Recent variability of the global ocean carbon sink. *Global Biogeochemical Cycles*, *28*(9), 927-949. doi: https://doi.org/10.1002/2014GB004853

Landschützer, P., Gruber, N., Haumann, F. A., Rödenbeck, C., Bakker, D. C. E., van Heuven, S., ... Wanninkhof, R. (2015). The reinvigoration of the southern ocean carbon sink. *Science*, *349*(6253), 1221-1224. doi: 10.1126/science.aab2620

Landschützer, P., Laruelle, G. G., Roobaert, A., & Regnier, P. (2020). A uniform pCO_2 climatology combining open and coastal oceans. *Earth System Science Data*, *12*(4), 2537-2553.

Le Quéré, C., Aumont, O., Monfray, P., & Orr, J. (2003). Propagation of climatic events on ocean stratification, marine biology, and CO_2: Case studies over the 1979–1999 period. *Journal of Geophysical Research: Oceans*, *108*(C12).

Le Quéré, C., Rödenbeck, C., Buitenhuis, E. T., Conway, T. J., Langenfelds, R., Gomez, A., ... others (2007). Saturation of the Southern Ocean CO_2 sink due to recent climate change. *Science*, *316*(5832), 1735–1738.

Lovenduski, N., Gruber, N., & Doney, S. C. (2008). Toward a mechanistic understanding of the decadal trends in the Southern Ocean carbon sink. *Global Biogeochemical Cycles*, *22*, GB3016.

Lovenduski, N., Gruber, N., Doney, S. C., & Lima, I. D. (2007). Enhanced CO_2 outgassing in the Southern Ocean from a positive phase of the Southern Annular Mode. *Global Biogeochemical Cycles*, *21*(2), GB2026.

Maritorena, S., d'Andon, O. H. F., Mangin, A., & Siegel, D. A. (2010). Merged satellite ocean color data products using a bio-optical model: Characteristics, benefits and issues. *Remote Sensing of Environment*, *114*(8), 1791-1804. doi: https://doi.org/10.1016/j.rse.2010.04.002

McKinley, G. A., Fay, A. R., Eddebbar, Y. A., Gloege, L., & Lovenduski, N. S. (2020). External forcing explains recent decadal variability of the ocean carbon sink. *AGU Advances*, *1*(2), e2019AV000149. doi: https://doi.org/10.1029/2019AV000149

McKinley, G. A., Fay, A. R., Lovenduski, N. S., & Pilcher, D. J. (2017). Natural variability and anthropogenic trends in the ocean carbon sink. *Annual review of marine science*, *9*, 125–150.

McKinley, G. A., Follows, M. J., & Marshall, J. (2004). Mechanisms of air-sea CO_2 flux variability in the equatorial Pacific and the North Atlantic. *Global Biogeochemical Cycles*, *18*(2).

Paulsen, H., Ilyina, T., Six, K. D., & Stemmler, I. (2017). Incorporating a prognostic representation of marine nitrogen fixers into the global ocean biogeochemical model HAMOCC. *Journal of Advances in Modeling Earth Systems*, *9*(1), 438 - 464.

Peters, G. P., Quéré, C. L., Andrew, R. M., Canadell, J. G., Friedlingstein, P., Ilyina, T., … Tans, P. (2017). Towards real-time verification of CO_2 emissions. *Nature Climate Change*, *7*(12), 848-850.

Raupach, M. R., Davis, S. J., Peters, G. P., Andrew, R. M., Canadell, J. G., Ciais, P., … Le Quere, C. (2014). Sharing a quota on cumulative carbon emissions. *Nature Climate Change*, *4*(10), 873–879.

Rayner, N. A., Parker, D. E., Horton, E. B., Folland, C. K., Alexander, L. V., Rowell, D. P., … Kaplan, A. (2003). Global analyses of sea surface temperature, sea ice, and night marine air temperature since the late nineteenth century. *Journal of Geophysical Research: Atmospheres*, *108*(D14). doi: https://doi.org/10.1029/2002JD002670

Resplandy, L., Keeling, R. F., Rödenbeck, C., Stephens, B. B., Khatiwala, S., Rodgers, K. B., … Tans, P. P. (2018). Revision of global carbon fluxes based on a reassessment of oceanic and riverine carbon transport. *Nature Geoscience*, *11*(7), 504-509.

Resplandy, L., Séférian, R., & Bopp, L. (2015). Natural variability of CO_2 and O_2 fluxes: What can we learn from centuries-long climate models simulations? *Journal of Geophysical Research: Oceans*, *120*(1), 384–404.

Reynolds, R. W., Rayner, N. A., Smith, T. M., Stokes, D. C., & Wang, W. (2002). An improved in situ and satellite SST analysis for climate. *Journal of Climate*, *15*(13), 1609–1625.

Ridge, S. M., & McKinley, G. A. (2021). Ocean carbon uptake under aggressive emission mitigation. *Biogeosciences*, *18*(8), 2711–2725.

Ritter, R., Landschützer, P., Gruber, N., Fay, A., Iida, Y., Jones, S., … others (2017). Observation-based trends of the Southern Ocean carbon sink. *Geophysical Research Letters*, *44*(24), 12–339.

Rödenbeck, C., DeVries, T., Hauck, J., Le Quéré, C., & Keeling, R. (2021). Data-based estimates of interannual sea–air CO_2 flux variations 1957–2020 and their relation to environmental drivers. *Biogeosciences Discussions*, *2021*, 1–43. doi: 10.5194/bg-2021-304

Rödenbeck, C. (2005). *Estimating CO_2 sources and sinks from atmospheric mixing ratio measurements using a global inversion of atmospheric transport* (Tech. Rep. No. 6). Max Planck Institute for Biogeochemistry, Jena. Retrieved from `http://www.bgc-jena.mpg.de/CarboScope/`

Rödenbeck, C., Keeling, R. F., Bakker, D. C. E., Metzl, N., Olsen, A., Sabine, C., & Heimann, M. (2013). Global surface-ocean pCO_2 and sea-air CO_2 flux variability from an observation-driven ocean mixed-layer scheme. *Ocean Science*, *9*(2), 193 - 216.

Schwinger, J., Goris, N., Tjiputra, J. F., Kriest, I., Bentsen, M., Bethke, I., … Heinze, C. (2016). Evaluation of NorESM-OC (versions 1 and 1.2), the ocean carbon-cycle stand-alone configuration of the Norwegian Earth System Model (NorESM1). *Geoscientific Model Development*, *9*(8), 2589–2622. doi: 10.5194/gmd-9-2589-2016

Sweeney, C., Gloor, E., Jacobson, A. R., Key, R. M., McKinley, G., Sarmiento, J. L., & Wanninkhof, R. (2007). Constraining global air-sea gas exchange for CO_2 with recent bomb 14C measurements. *Global Biogeochemical Cycles*, *21*(2).

Taylor, K. E. (2001). Summarizing multiple aspects of model performance in a single diagram. *Journal of Geophysical Research: Atmospheres*, *106*(D7), 7183-7192. doi: https://doi.org/10.1029/2000JD900719

Wanninkhof, R. (1992). Relationship between wind speed and gas exchange over the ocean. *Journal of Geophysical Research: Oceans*, *97*(C5), 7373-7382. doi: https://doi.org/10.1029/92JC00188

Supporting Information for "Observation-based variability in the global ocean carbon sink from 1959-2020"

Val Bennington[1,2], Lucas Gloege[3], Galen A McKinley[1]

[1]Lamont-Doherty Earth Institute, Columbia University

[2]Makai Ocean Engineering, Inc.

[3]NASA-GISS

Contents of this file

Corresponding author: Val Bennington, Makai Ocean Engineering, Inc. Hawaii, USA. (Valerie.Bennington@makai.com)

S1. Reconstructed Air-Sea CO_2 Fluxes

Figure S1 shows the air-sea CO_2 fluxes reconstructed by LDEO-HPD as compared to the eight GOBMs and HPD Climatology Test (Figure S1 a), Jena MLS (Figure S1 b), other observation-based products (Figure S1 c) and the box model simulations with and without volcanoes (McKinley et al., 2020) (Figure S1 d).

S2. Anomalies of Detrended Reconstructed Air-Sea CO_2 Fluxes

Figure S2 shows the anomalies of detrended air-sea CO_2 fluxes in the four ocean basins. The years of major volcanic eruptions are depicted with vertical grey lines Agung (1963), El Chichon (1982) and Mt. Pinatubo (1991). The Pacific and Southern Oceans show clear increases in their ocean sink immediately following the volcanic eruptions.

References

McKinley, G. A., Fay, A. R., Eddebbar, Y. A., Gloege, L., & Lovenduski, N. S. (2020). External forcing explains recent decadal variability of the ocean carbon sink. *AGU Advances*, *1*(2), e2019AV000149. doi: https://doi.org/10.1029/2019AV000149

Rödenbeck, C., DeVries, T., Hauck, J., Le Quéré, C., & Keeling, R. (2021). Data-based estimates of interannual sea–air co$_2$ flux variations 1957–2020 and their relation to environmental drivers. *Biogeosciences Discussions*, *2021*, 1–43. doi: 10.5194/bg-2021-304

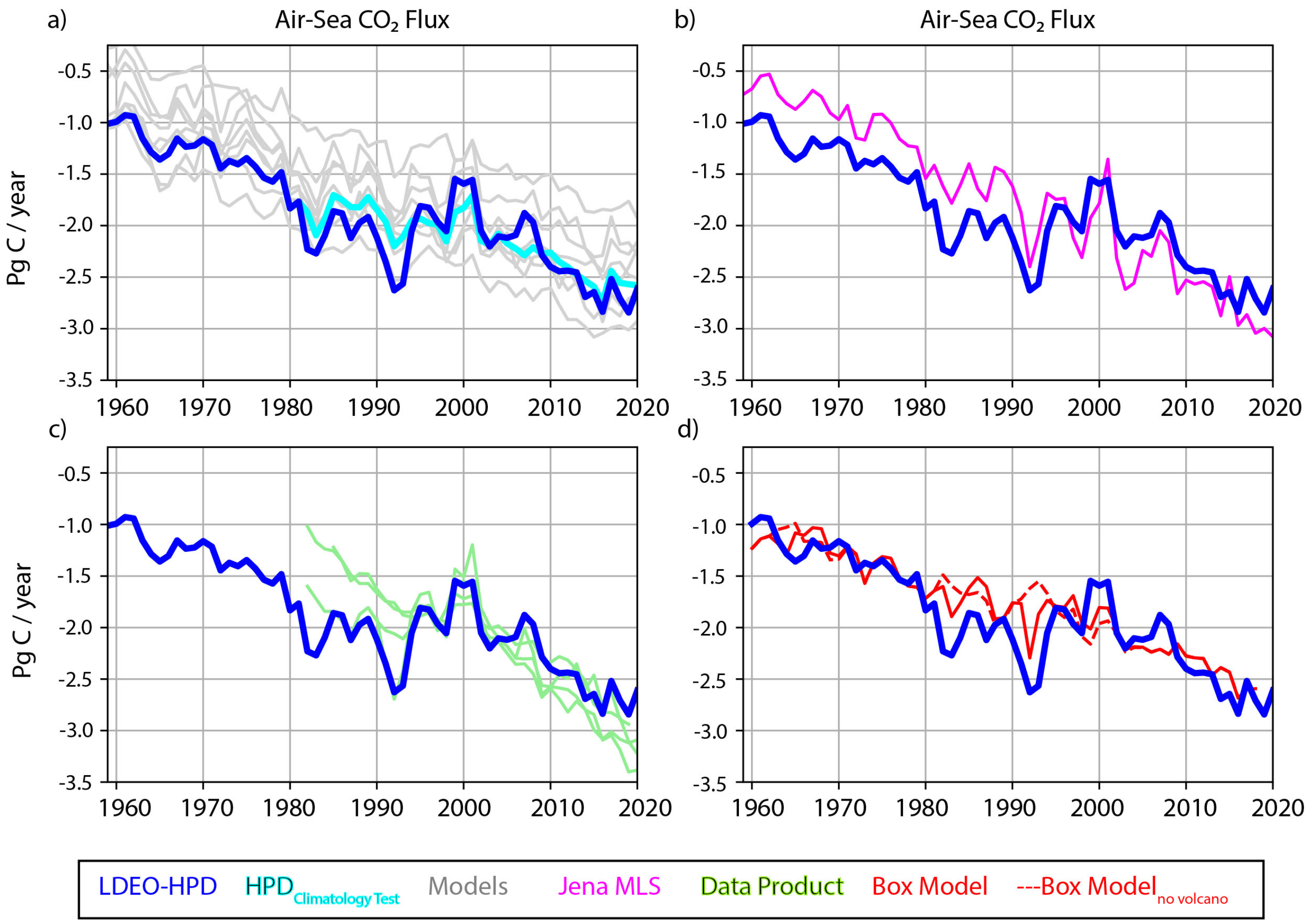

Figure S1. (a) Air-sea CO_2 fluxes for 1959-2020 according to LDEO-HPD (blue), HPD Climatology Test (cyan), and the nine unadjusted GOBMs (grey). (b) Air-sea CO_2 fluxes for 1959-2020 according to LDEO-HPD (blue) and Jena MLS (magenta) (Rödenbeck et al., 2021). (c) Air-sea CO_2 fluxes for 1959-2020 according to LDEO-HPD (blue) and the other data products (green). (d) Air-sea CO_2 fluxes for 1960-2018 according to LDEO-HPD (blue) and the box model of McKinley et al. (2020) with volcanoes (red) and without volcanoes (dashed red).

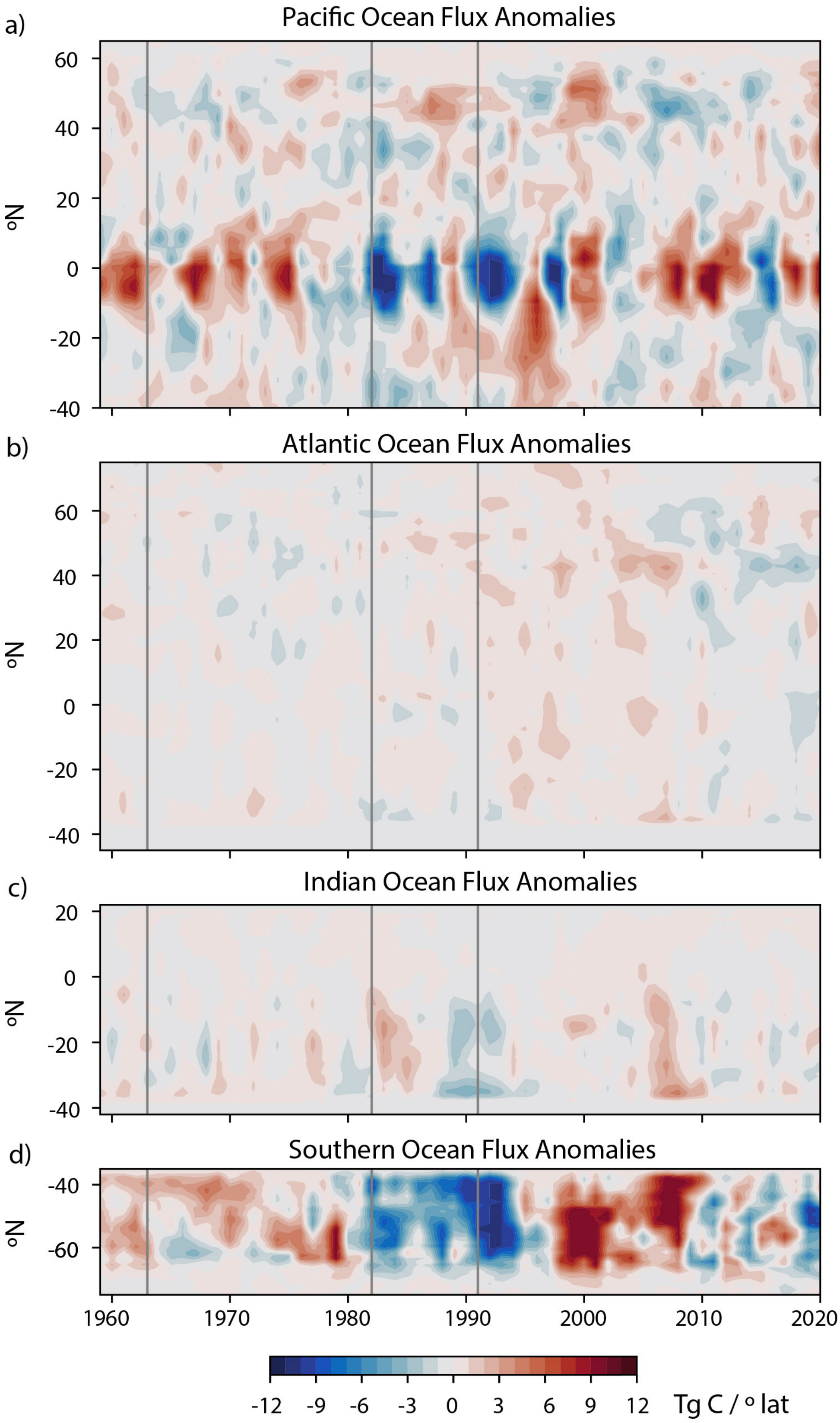

Figure S2. Detrended air-sea CO_2 flux anomalies in four ocean basins (TgC/yr/^{o}lat). Major volcanic eruptions denoted with vertical grey lines (Agung, March 1963; Chichon, April 1982; Pinatubo, June 1991).

March 9, 2022, 9:45pm